

# $K^-$ - nucleus relativistic mean field potentials consistent with kaonic atoms

E. Friedman<sup>a</sup>, A. Gal<sup>a</sup>, J. Mares<sup>b</sup>, A. Cieplý<sup>a,b</sup>

<sup>a</sup>*Racah Institute of Physics, The Hebrew University, Jerusalem 91904, Israel*

<sup>b</sup>*Nuclear Physics Institute, 25068 Řež, Czech Republic*

## Abstract

$K^-$  atomic data are used to test several models of the  $K^-$  nucleus interaction. The  $t(\rho)\rho$  optical potential, due to coupled channel models incorporating the  $\Lambda(1405)$  dynamics, fails to reproduce these data. A standard relativistic mean field (RMF) potential, disregarding the  $\Lambda(1405)$  dynamics at low densities, also fails. The only successful model is a hybrid of a theoretically motivated RMF approach in the nuclear interior and a completely phenomenological density dependent potential, which respects the low density theorem in the nuclear surface region. This best-fit  $K^-$  optical potential is found to be strongly attractive, with a depth of  $180\pm 20$  MeV at the nuclear interior, in agreement with previous phenomenological analyses.

*PACS:* 24.10.Ht; 36.10.Gv

January 1, 2018

## I. INTRODUCTION

The interaction and properties of  $K^-$  mesons in nuclear matter have attracted considerable attention in the last few years, as may be gathered from the recent reviews in the Dover memorial volume of Nuclear Physics A [1–3] and the references cited therein. Among the topics discussed was the question of kaon condensation [4] in dense nuclear matter and the possibility of the onset of such condensation in neutron stars [5–7]. Formation of the condensate would soften the equation of state of baryonic matter and consequently would reduce the upper limit for the mass of neutron stars. Such scenarios depend on the depth of the attractive  $K^-$  optical potential at normal nuclear densities where experimental information is available.

Theoretical considerations based on One Boson Exchange (OBE) models, coupled channel chiral perturbation theory approach, or Relativistic Mean Field (RMF) models, yield for the attractive real part of the  $K^-$  nucleus potential at threshold depths in the range between 70 and 120 MeV [1–3]. The reason for such a spread of the predicted values lies in the diversity of treating the  $\Lambda(1405)$  hyperon, which is considered to be an unstable  $\bar{K}N$  bound state just below the  $K^-p$  threshold. The purpose of the present work is to test some of these  $K^-$  nucleus interaction models by confronting these models with kaonic atom data. This is particularly topical, since recent fits [8,9] to the  $K^-$  atomic data using a purely phenomenological nonlinear density dependent (DD) optical potential yield a rather different value for its real part in the nuclear interior,  $\text{Re } V_{opt} = -200 \pm 20$  MeV. The effect of the  $\Lambda(1405)$  is taken into account in these fits implicitly by imposing the low density theorem.

In Sec. II we briefly review the phenomenological fit to the  $K^-$  atomic data using a DD optical potential [8,9]. The results of applying the chirally motivated coupled channel approach due to Weise and collaborators [10,11] are discussed in Sec. III. We find that this microscopic model, in its present form, fails to reproduce satisfactorily the  $K^-$  atomic data, in spite of the correct low density limit which is ensured by its success to reproduce the  $\Lambda(1405)$  dominance of the near-threshold  $K^-p$  physics. In Sec. IV we describe the application of the RMF approach, in which the choice of the scalar and vector couplings is motivated by SU(3) and by the quark model. This approach, which violates the low density limit by disregarding the  $\Lambda(1405)$ , also fails to reproduce satisfactorily the  $K^-$  atomic data. A good fit to the  $K^-$  atomic data can be made only at the expense of a large departure of the fitted RMF scalar and vector couplings from their underlying theoretical values. Finally, in Sec. V we introduce a hybrid model which combines the RMF potential form in the nuclear interior with a phenomenological DD form at low density. We show that within this model, and respecting the low density limit, it is possible to fit reasonably well the atomic data with only a moderate departure from the theoretically motivated RMF couplings. The results of this work are summarized and discussed in Sec. VI.

## II. DENSITY DEPENDENCE: PHENOMENOLOGY

The interaction of  $K^-$  with the nucleus is described by the Klein-Gordon (KG) equation of the form presented in Ref. [12]:

$$\left[ \nabla^2 + k^2 - 2\varepsilon(k)(V_{opt} + V_c) + V_c^2 \right] \phi = 0 \quad (\hbar = c = 1) \quad (1)$$

where  $k$  and  $\varepsilon(k)$  are the  $K^-$  - nucleus wave number and reduced energy in the c.m. system, respectively, and  $V_c$  is the Coulomb interaction of the  $K^-$  with the nucleus. The phenomenological DD potential of Friedman *et al.* [8,9] is given at threshold by:

$$2\mu V_{opt}(r) = -4\pi(1 + \frac{\mu}{m})b(\rho)\rho(r) \quad , \quad (2)$$

$$b(\rho) = b_0 + B_0(\frac{\rho(r)}{\rho_0})^\alpha \quad , \quad (3)$$

where  $\mu$  is the  $K^-$ -nucleus reduced mass,  $b_0$  and  $B_0$  are complex parameters determined from fits to the data,  $m$  is the mass of the nucleon and  $\rho(r) = \rho_n(r) + \rho_p(r)$  is the nuclear density distribution normalized to the number of nucleons  $A$ , and  $\rho_0 = 0.16 \text{ fm}^{-3}$  is a typical central nuclear density. For  $\alpha > 0$  and  $\rho \rightarrow 0$ , the second term on the r.h.s. of Eq. (3) vanishes and the optical potential of Eq. (2) assumes the  $t\rho$  form. Furthermore, for  $b_0 = -0.15 + i0.62 \text{ fm}$  (equal to minus the free  $K^-N$  scattering length) the low density limit is satisfied, so that the potential is repulsive in the low density region, reflecting the presence of the subthreshold  $\Lambda(1405)$  unstable bound state. Since any fit to the data yields  $\text{Re}(B_0 + b_0) > 0$ , such potentials become attractive in the nuclear interior. For the best-fit DD potential, the transition from repulsion to attraction occurs near  $\rho/\rho_0 = 0.15$ , the depth of this attractive  $V_{opt}$  at  $\rho_0$  is then about 190 MeV. For a detailed discussion of the DD potentials as well as of the  $\chi^2$  fits to the kaonic atom data see Ref. [12]. Here we note only that the full data base for kaonic atoms, containing 65 data points over the whole of the periodic table, was used in the fits, which yielded  $\chi^2$  per point around 1.5, representing good fits to the data. Such fits will serve as a reference to the quality of fits attainable with other models, as is discussed below. For comparison we note that the best fit (everywhere attractive)  $t\rho$  potential is considerably shallower than the best fit DD, but with  $\chi^2/N \approx 2.0$  it is also significantly inferior to the latter.

### III. DENSITY DEPENDENCE: THEORY

Weise and collaborators (for a recent review see Ref. [1]) iterated the lowest order chiral effective interaction between the pseudoscalar meson octet and the baryon octet in a Lippmann-Schwinger (LS) coupled channel matrix equation. For  $S = -1$ , the parameters of the model were fitted [10] to both the low energy  $\bar{K}N$  observables and to the  $\pi\Sigma$  spectrum which provides the major evidence for the  $I=0$   $\Lambda(1405)$   $\bar{K}N$  unstable bound state 27 MeV below the  $K^-p$  threshold. The LS coupled channel equations were then solved in the nuclear medium [11], taking into account the Pauli exclusion principle in the intermediate nucleon states, as a function of the Fermi momentum  $p_F$  within the Fermi gas model. Fermi motion and nucleon binding effects were also considered, but turned out to play only a secondary role. We have reproduced in the present work this calculation and Fig. 1 shows the in-medium isospin-averaged  $\bar{K}N$  threshold scattering amplitude  $b$ , which is a function of the corresponding local nuclear density  $\rho$ . It is instructive to plot  $b(\rho)$  as a function of position for a hypothetical nucleus with density represented by a Fermi function with a radius parameter of 5 fm, a diffuseness parameter of 0.5 fm, and a central density of  $0.16 \text{ fm}^{-3}$ . The

$K^-$  nucleus optical potential, for a self-conjugate ( $N = Z$ ) nucleus, is then given by Eq. (2) in terms of  $b(\rho)$ .

It is clear from Fig. 1 that  $\text{Re } V_{opt}$  changes from repulsion (due to the subthreshold  $\Lambda(1405)$ ) in the limit of  $\rho=0$ , where it satisfies the low density theorem with  $b(\rho = 0)$  given by the free-space  $\bar{K}N$  threshold scattering amplitude, to attraction beginning near  $\rho/\rho_0 = 0.1$ , where  $\rho_0 = 0.16 \text{ fm}^{-3}$ . The depth of this attractive real potential at  $\rho_0$  is then about 120 MeV. These observations remain in place also when refined variants [13,14] of the model are used.

For  $\text{Im } V_{opt}$ , which is due to the one-nucleon absorption processes  $K^- N \rightarrow \pi Y$ , we note that it deviates significantly from linearity in the density  $\rho$ , precisely at the low density region where  $\text{Re } V_{opt}$  changes sign, owing to the resonance-like form of  $\text{Im } b(\rho)$ . This is the density region where the coupled channel generated  $\Lambda(1405)$  moves through the  $K^-$  threshold and, therefore, it is there where it exercises a strong influence on the  $K^-$  atomic states.

For nuclei with  $N > Z$ , the generic form  $b(\rho)\rho(r)$  in the potential (2) actually stands for  $b_p(\rho_p)\rho_p(r) + b_n(\rho_n)\rho_n(r)$ . This more general potential was used in the KG equation (1) to evaluate  $K^-$  atomic shifts and widths for the same data set employed in Sec. II. The value of  $\chi^2$  per point is then close to 15, representing very poor agreement between predictions and experiment. Applying fudge factors to the density dependent amplitudes we can obtain reasonably good fits to the data only at the expense of introducing unphysically large modifications of the elementary amplitudes, e.g. by a factor of 0.1 for the  $K^-p$  and by a factor of 2.4 for the  $K^-n$  interactions. The results are essentially unchanged if we use the present microscopic approach only for the real potential while employing a phenomenological approach for the imaginary potential, or vice versa. It is therefore concluded that although the correct low density behavior is built into the model, consistently with the effects of the  $\Lambda(1405)$  resonance, this microscopic model fails to describe the interaction of  $K^-$  with nuclei at threshold. Comparing the optical potential of this model to the successful purely phenomenological model of Sec. II, it is apparent that fitting to the data excludes a sizable enhancement of  $\text{Im } b(\rho)$  in the outer nuclear surface and, furthermore, the presence of two distinct extrema of  $\text{Re } b(\rho)$  in this region.

#### IV. RELATIVISTIC MEAN FIELD

In the derivation of  $\text{Re } V_{opt}$  within the RMF approach we make use of the standard Lagrangian for the nucleons with the linear parametrization (L) of Horowitz and Serot [15]. For comparison, we quote below results also for the non-linear parametrization (NL1) due to Reinhard *et al.* [16]. The antikaon sector is incorporated into the model by using the Lagrangian density of the form [7]:

$$\mathcal{L}_K = \partial_\mu \bar{\psi} \partial^\mu \psi - m_K^2 \bar{\psi} \psi - g_{\sigma K} m_K \bar{\psi} \psi \sigma - i g_{\omega K} (\bar{\psi} \partial_\mu \psi \omega^\mu - \psi \partial_\mu \bar{\psi} \omega^\mu) + (g_{\omega K} \omega_\mu)^2 \bar{\psi} \psi. \quad (4)$$

The Lagrangian  $\mathcal{L}_K$  describes the interaction of the antikaon field ( $\bar{\psi}$ ) with the scalar ( $\sigma$ ) and vector ( $\omega$ ) isoscalar fields. The corresponding equation of motion for  $K^-$  in a  $Z = N$  nucleus can be expressed by the KG equation (1) with the real part of the optical potential given at threshold by:

$$\text{Re } V_{opt} = \frac{m_K}{\mu} \left( \frac{1}{2} S - V - \frac{V^2}{2m_K} \right) \quad , \quad (5)$$

where  $S = g_{\sigma K} \sigma(r)$  and  $V = g_{\omega K} \omega_0(r)$  in terms of the mean isoscalar fields. Similar considerations have been made recently for the interaction of kaons with nuclei [17]. Note that for antikaons, the vector potential  $V$  contributes attraction, just opposite to its role for kaons and nucleons. Each of the three terms on the r.h.s. of Eq. (5), thus, gives rise to attraction. Consequently, it becomes impossible to satisfy the low density limit which requires that, due to the subthreshold  $\Lambda(1405)$ ,  $\text{Re } V_{opt} > 0$  as  $\rho \rightarrow 0$ . For nuclei with  $N > Z$ , the potential should include also an isovector part due to the interaction of the  $K^-$  with the  $\rho$  meson field. However, this was omitted from the present calculations as it was found to have marginal effect in previous analyses of kaonic atoms [8,9,12].

In order to avoid calculating RMF real potentials for the 24 different nuclei contained in the full kaonic atoms data base [9], we have first confirmed that using a reduced data set of only 11 points for carefully selected four atoms, namely O, Si, Ni and Pb, produces all the features observed in the potentials obtained from fits to the full data set, in agreement with the results shown in Table 2 of Ref. [18]. As a guide we used fits of the phenomenological DD potential of Sec. II to this reduced data set. Since the RMF approach does not address the imaginary part of the potential, the latter has to be treated on a more empirical basis, as done for example in recent RMF treatments of hyperon-nucleus interactions at intermediate energies [19], and of  $\Sigma^-$  atoms [20]. Therefore, for RMF real potentials of the form (5), the imaginary part of Eq. (2) was used within a phenomenological DD form, and also within the microscopic approach of Sec. III, and its parameters were fitted to the data.

In order to construct the RMF  $\text{Re } V_{opt}$  of Eq. (5) in terms of the scalar  $S$  and the vector  $V$  potentials, one needs to specify  $\alpha_\sigma$  and  $\alpha_\omega$ , where  $\alpha_m = g_{mK}/g_{mN}$ . The quark model (QM) choice  $\alpha_\sigma = \alpha_\omega = \frac{1}{3}$ , as expected from naively counting the nonstrange quarks in the  $\bar{K}$  with respect to those in the nucleon [21], leads to a very poor fit to the data, as is clearly seen in Table I for this RMF-in potential (other parametrizations of  $\text{Im } V_{opt}$  led to invariably poor fits). Therefore, in the next stage, we treated both  $\alpha_\sigma$  and  $\alpha_\omega$  as free parameters and searched for their best fit values. In this particular case, the effects of the  $\Lambda(1405)$  which are expected at low densities, are not included *a priori*. The best fit potential (denoted by RMF-fit in Table I) consists of a strongly attractive vector potential and a strongly *repulsive* scalar potential (note the minus sign for  $\alpha_\sigma$ ). The optical potential  $\text{Re } V_{opt}$  corresponding to these coupling ratios is attractive in the nuclear interior with the depth of about 190 MeV, in close agreement with the DD potentials [12]. The solid curve in Fig. 2 shows this best fit RMF(L) potential for Ni. Also shown in this figure are the DD potential for this example of Ni and the QM input RMF(L) potential with  $\alpha_\omega = \alpha_\sigma = \frac{1}{3}$ . The best fit RMF potential is steeper in the surface region than the input RMF potential, and it becomes, in fact, repulsive at large radii. Kaonic atoms data thus force the RMF potential to *qualitatively* satisfy the low density limit of being repulsive at large radii. The sizable departure of the fitted values of the parameters  $\alpha_\sigma$  and  $\alpha_\omega$  from those of the input QM values, as well as the sharp decrease of  $\chi^2/N$  associated with the RMF fit (see Table I), reflect *a posteriori* effects of the  $\Lambda(1405)$  at low densities. Various choices for the functional form of  $\text{Im } V_{opt}$  were tried, leading to qualitatively similar results regarding the reversal of  $S(r)$  from attraction to repulsion. The imaginary part of the potential used in the RMF fits specified in Table I and shown in Fig. 2 was taken in the  $t\rho$  form. It is also seen from Table I that  $\text{Im } V_{opt}$

is well determined for the RMF-fit potential, with a depth of about 60 MeV, close to the value expected from the low density limit. This feature remained essentially unchanged in the subsequent fits discussed below.

## V. HYBRID MODEL

The existence of the  $\Lambda(1405)$  resonance poses a difficulty for the RMF approach if the parameters  $\alpha_m$  are allowed to deviate only moderately from the values suggested by the underlying hadron symmetries. It is also clear that a mean field model cannot be applied reliably in the low density region where the  $K^-$  interaction with the nuclear medium is affected by the  $\Lambda(1405)$ . In this region, since no theoretical model has been shown to be successful, we adopted the DD potential of Friedman *et al.* [8,9], as described in Sec. II, which takes the effect of the  $\Lambda(1405)$  hyperon into account at least phenomenologically by imposing the low density limit. On the other hand the RMF description is well justified within the nuclear interior, for densities larger than about  $0.2\rho_0$ , where the effect of  $\Lambda(1405)$  can be neglected as demonstrated in Refs. [11,22]. We have therefore combined the two approaches into a hybrid model as follows.

In the hybrid model, the functional RMF form Eq. (5) is used in the nuclear interior for  $\text{Re } V_{opt}$ , whereas the purely phenomenological DD form Eq. (2) is used in the surface of the nucleus and beyond. The radius  $R_M$  where the two forms are matched to each other is chosen as  $R_M \approx R_{1/2} + 0.1$  fm, where  $\rho(R_{1/2}) = \rho_0/2$ . The sensitivity to the choice of  $R_M$  was checked and found to be small. The value chosen corresponds to the minimal spread of the fitted coupling constant ratio  $\alpha_\sigma$  for the various nuclei. The density  $\rho(R_M)$  is sufficiently high to justify using the RMF approach, and sufficiently low so that the atomic data are still sensitive to the RMF form. Figure 4 of Ref. [12], and in particular Fig. 3 of Ref. [18] for Ni, show that by analyzing kaonic atoms one determines the real part of the  $K^-$  nucleus DD optical potential up to  $\rho = 0.9\rho_0$ . This is well above the density at which the RMF form takes over in the present approach.

Fitting to the  $K^-$  atomic data, the RMF vector coupling constant ratio  $\alpha_\omega$  was kept fixed, guided by theoretical considerations, and the RMF scalar coupling constant ratio  $\alpha_\sigma$  was varied together with the parameters of the DD real potential form (for  $r > R_M$ ). For the imaginary potential, since the RMF approach does not provide any specific prescription, the purely phenomenological DD potential form was used throughout. For the coupling constant  $g_{\omega K}$  we used either the constituent QM value  $\alpha_\omega = \frac{1}{3}$ , or the SU(3) relation  $2g_{\omega K} = g_{\rho\pi} = 6.04$  (denoted by SU(3) in Table I). Table I shows that the various hybrid RMF+DD potentials describe the data reasonably well with  $\chi^2/N$  values of 1.4 – 1.5.

Figure 3 shows the hybrid RMF(L)+DD best fit real potentials for Ni, for the QM and SU(3) options. The DD potential is also shown, for comparison. It is seen that the depths of the hybrid real potentials in the nuclear interior for the different values of  $\alpha_\omega$  are about 185 MeV and are very close to each other, and also to the depth of the purely phenomenological DD potential. We note that omitting the  $V^2$  term in Eq. (5), and refitting the  $K^-$  atomic data, the resulting depths are smaller than the RMF(L)+DD depths shown in Fig. 3 by less than 10 MeV.

Figure 4 shows the dependence of the RMF+DD best fit real potentials for Pb on the type of RMF model used: the linear model L [15], and the nonlinear models NL1 [16] and

NLS [23]. The latter nonlinear model, due to Sharma *et al.*, was shown [24] to fit particularly well the Pb isotopes, and it is therefore gratifying that it yields a very similar  $V_{opt}$  to that for the linear model. The QM value  $\alpha_\omega = 1/3$  was used throughout these best fit potentials.

It is interesting to note the following expression for the  $\bar{K}$  real potential (attractive) depth,

$$U^{(\bar{K})} = \frac{1}{2}\alpha_\sigma U_S^{(N)} + \alpha_\omega U_V^{(N)} + \frac{(\alpha_\omega U_V^{(N)})^2}{2m_K} \quad , \quad (6)$$

in terms of the nucleon vector and scalar potential depths, respectively, which for the linear model L in the mean field approximation are given by

$$U_V^{(N)} = \rho_V \frac{g_{\omega N}^2}{m_\omega^2} \quad , \quad U_S^{(N)} = \rho_S \frac{g_{\sigma N}^2}{m_\sigma^2} \quad , \quad (7)$$

where  $\rho_V$  and  $\rho_S$  are the nuclear vector and scalar densities, respectively, evaluated at nuclear matter density. Analogous expressions for the potential depths of hyperons in nuclear matter were discussed in Refs. [25,26]. For  $\rho_V = \rho_0$  and  $\rho_S = 0.9\rho_0$ , with  $\rho_0 = 0.16 \text{ fm}^{-3}$ , Eq. (6) yields for model L:

$$U^{(\bar{K})} = 189 \text{ MeV (QM)} \quad , \quad 181 \text{ MeV (SU(3))} \quad , \quad (8)$$

in excellent agreement with the results of the fits shown in Figs. 3 and 4. Thus, for a given model for  $\alpha_\omega$ , fitting to the  $K^-$  atomic data yields a value for  $\alpha_\sigma$  which results in  $U^{(\bar{K})} \approx 185 \text{ MeV}$ . This depth  $U^{(\bar{K})}$  clearly has more physical content than the separate values  $\alpha_m$ , given in Table I for the coupling-constant ratios. We note in passing that this approximate model independence of  $U^{(\bar{K})}$  is not shared by the ( $S=1$ ) K-nucleus potential depth  $U^{(K)}$  which can be derived from Eq. (6) reversing the sign of  $\alpha_\omega$ . The QM choice yields 66 MeV *repulsive* depth, whereas the SU(3) choice yields 14 MeV *attractive* depth. Allowing  $\alpha_\omega$  to depart moderately, say, from the QM value, it is possible to get a comparable  $K^-$  atomic fit which yields a repulsive depth  $U^{(K)}$  at threshold of about 30 MeV, as expected from the scattering length approximation (see Eq. (11) of Ref. [2]). The value of  $U^{(\bar{K})}$  for this fit remains remarkably close to the value given by Eq. (8).

The present values of  $\alpha_\omega$  and  $\alpha_\sigma$  are not directly related to the ones encountered in calculations of two-body  $KN$  phase shifts. For example, the OBE potential model A of Büttgen *et al.* [27], which uses the Bonn potential coupling constants  $g_{mN}$  in the nucleonic sector, treats  $\alpha_\omega$  and  $\alpha_\sigma$  as free parameters. Although their value of  $\alpha_\omega = 0.312$  is very close to the QM value  $\frac{1}{3}$  adopted here in one of the hybrid model fits, the magnitude of  $g_{\omega N}$  is somewhat larger in their calculation than that used in the RMF calculation of Horowitz and Serot [15] adopted in the present work. Hence the vector contribution to  $U^{(\bar{K})}$  would be correspondingly larger than the vector contribution in our calculations. However, their value of  $\alpha_\sigma = 0.158$  is considerably smaller than the values obtained in our hybrid model fits, so that the scalar contribution to  $U^{(\bar{K})}$  is almost negligible, less than 20 MeV, for their parameters. Altogether, the parameters of model A of Ref. [27] would yield  $U^{(\bar{K})} = 175 \text{ MeV}$ , fortuitously close to our hybrid model fit values of Eq. (8). Subsequent studies by the Jülich group of the  $\bar{K}N$  system [28] and of the  $KN$  system [29] relied on model B of Ref. [27], using an additional scalar meson exchange with unspecified G-parity nature. It is beyond the scope of the present paper to discuss these works.

## VI. CONCLUSION

To summarize, by testing several models of the  $K^-$  nucleus interaction, we have found that only the hybrid model RMF+DD optical potentials lead to a good agreement with the existing atomic data. These potentials have an attractive real part in the nuclear interior with a depth of  $180\pm 20$  MeV. This result confirms previous phenomenological DD analyses [8,9,12] where the density dependent potentials are constrained to respect the low density limit, thus including implicitly effects of the  $\Lambda(1405)$  resonance.

The failure of the chirally motivated coupled channel model [10] to produce reasonable agreement with the  $K^-$  atomic data is disturbing, since the input free space  $t(\rho=0)$  to the  $K^-$  nucleus potential  $V_{opt} = t(\rho)\rho$  is constrained in this model by the available low energy  $\bar{K}N$  experimental data. Recall that the model generates dynamically the subthreshold  $\Lambda(1405)$  unstable bound state which is believed to dominate the low energy  $K^-p$  physics. The parameters used in Ref. [11] have been updated in Ref. [13]; furthermore, the  $\bar{K}N - \pi Y$  coupled channel model [10] has been recently extended to include also  $\eta Y$  and  $K\Xi$  channels [14]. Yet, the depth of the resulting  $K^-$  nucleus optical potential has remained low, about 100 MeV according to Ref. [30]. However, the spectacular failure of the chirally motivated coupled channel models ( $\chi^2/N \approx 15$ ) cannot be linked just to the depth of the potential in the nuclear interior, since the  $t\rho$  potential which fits relatively well ( $\chi^2/N \approx 2$ ) the  $K^-$  atomic data is also found to have a depth of about 100 MeV [12]. In summary, it is fair to state that these model extrapolations of the  $\bar{K}N$  dynamics at threshold, from free space to finite density, fail to pass a quantitative test of  $K^-$  atoms.

The optical potential  $t(\rho)\rho$  is the first order term in a multiple scattering expansion of  $V_{opt}$  (e.g. Ref. [31]). Higher order terms are not necessarily negligible. The second order term is due to nuclear pair correlations and has been studied recently by two groups. Waas *et al.* [32] evaluated the effect of Pauli and of short range correlations and found it to be of a relatively medium sized *repulsive* nature. Pandharipande *et al.* [33], in a calculation geared to high density neutron stars, found larger repulsive contributions. The leading power of the density with which nuclear correlations affect  $V_{opt}$  is  $\rho^{4/3}$ . We note, however, that the purely phenomenological best fit DD Re  $V_{opt}$  specified in Table I is dominated in the nuclear interior by an *attractive*  $\rho^{4/3}$  term. Thus, the above two models [32,33] give rise to a considerably shallower  $K^-$  nucleus potential in the nuclear interior than the best fit DD potential. This discrepancy poses a major theoretical challenge. One cannot rule out that the multiple scattering conventional approach to  $V_{opt}$  breaks down for the  $K^-$  nucleus system, unless a self consistency requirement similar to that considered very recently by Lutz [34] is imposed on the  $K^-$  optical potential. However, this self-consistent treatment gives even shallower  $K^-$  nucleus potential than due to the coupled channel model of Refs. [10,11]. Finally, we mention attempts to construct microscopically the density dependence of  $V_{opt}$ , considering explicitly  $\Lambda(1405)$  degrees of freedom, by using a  $\Lambda(1405)$  particle - nucleon hole model for the nuclear excitations involved (Ref. [35] and references cited therein). Limited sets of  $K^-$  atomic data have been fitted in such models, at the expense of introducing new parameters that have to do with the hypothesized complex mean field experienced by the  $\Lambda(1405)$ . The simplest term that must be added to the underlying Lagrangian, in order to enforce such attempts, is an effective four Fermi interaction involving both  $N$  and  $\Lambda(1405)$ , with unknown coupling constant. The problematics of this approach are discussed in Sec. 5 of Ref. [32].



The failure of the RMF model, with couplings not too dissimilar to those motivated by the QM or SU(3), is less of a theoretical concern, since the resulting  $V_{opt}$  which is attractive everywhere ignores the effect of the  $\Lambda(1405)$  by violating the low density limit. It appears that a necessary condition for  $V_{opt}$  to produce a good agreement with the  $K^-$  atomic data is that it behaves properly at low density. This is the prime motivation for introducing the hybrid RMF+DD model in Sec. V. Previous applications of the RMF approach to the  $K^-$  sector ([2] and references cited therein plus, quite recently, the related quark meson coupling model calculation [36]) have not been meaningfully constrained by low energy  $\bar{K}N$  data. It is worth recalling in this context that the RMF nucleon couplings, also, do not follow directly from  $NN$  data, although they roughly follow from the Lorentz structure of several OBE  $NN$  potential models. However, for the RMF approach to assume a broad validity in hadronic physics, one would like the couplings in the  $S = -1$  strange sector to be related to those in the  $S=0$  nonstrange sector, as suggested by the underlying symmetries governing hadron structure, such as the QM and SU(3) used here. This harmonious viewpoint is only partially successful in RMF studies of hypernuclei [37] and of  $\Sigma^-$  atoms [20]. Similarly, for the coupling ratios determined by fitting the hybrid RMF+DD model to the  $K^-$  atomic data (Table I), moderate departures occur from a pure adherence to the QM, or to the SU(3) coupling ratios. We conclude that the hybrid model potentials represent the most theoretically inclined  $K^-$  nucleus potentials which are worth using for extrapolating into high density matter.

This research was partially supported by the Israel Science Foundation (E.F.), by the U.S.-Israel Binational Science Foundation (A.G.) and by the Grant Agency of the Czech Republic (A.C. and J.M., grant No. 2020442). J.M. acknowledges the hospitality of the Hebrew University. A.C. thanks T. Waas for useful information on the subject matter of Ref. [11].

## REFERENCES

- [1] T. Waas and W. Weise, Nucl. Phys. **A625**, 287 (1997).
- [2] J. Schaffner-Bielich, I.N. Mishustin, and J. Bondorf, Nucl. Phys. **A625**, 325 (1997).
- [3] G.Q. Li, C.H. Lee, and G.E. Brown, Nucl. Phys. **A625**, 372 (1997).
- [4] D.B. Kaplan and A.E. Nelson, Phys. Lett. B **175**, 57 (1986).
- [5] G.E. Brown, C.H. Lee, M. Rho, and V. Thorsson, Nucl. Phys. **A567**, 937 (1994).
- [6] V. Thorsson, M. Prakash, and J.M. Lattimer, Nucl. Phys. **A572**, 693 (1994).
- [7] J. Schaffner, A. Gal, I.N. Mishustin, H. Stoecker, and W. Greiner, Phys. Lett. B **334**, 268 (1994); J. Schaffner and I.N. Mishustin, Phys. Rev C **53**, 1416 (1996).
- [8] E. Friedman, A. Gal, and C.J. Batty, Phys. Lett. B **308**, 6 (1993).
- [9] E. Friedman, A. Gal, and C.J. Batty, Nucl. Phys. **A579**, 518 (1994).
- [10] N. Kaiser, P.B. Siegel, and W. Weise, Nucl. Phys. **A594**, 325 (1995).
- [11] T. Waas, N. Kaiser, and W. Weise, Phys. Lett. B **365**, 12 (1996); **379**, 34 (1996).
- [12] C.J. Batty, E. Friedman, and A. Gal, Phys. Rep. **287**, 385 (1997).
- [13] N. Kaiser, T. Waas, and W. Weise, Nucl. Phys. **A612**, 297 (1997).
- [14] E. Oset and A. Ramos, Nucl. Phys. **A635**, 99 (1998).
- [15] C.J. Horowitz and B.D. Serot, Nucl. Phys. **A368**, 503 (1981).
- [16] P.-G. Reinhard, M. Rufa, J. Maruhn, W. Greiner, and J. Friedrich, Z. Phys. A **323**, 13 (1986).
- [17] E. Friedman, A. Gal, and J. Mareš, Nucl. Phys. **A625**, 272 (1997).
- [18] E. Friedman, Nucl. Phys. **A639**, 511c (1998).
- [19] E.D. Cooper, B.K. Jennings, and J. Mareš, Nucl. Phys. **A580**, 419 (1994); *ibid.* **A585**, 157c (1995).
- [20] J. Mareš, E. Friedman, A. Gal, and B.K. Jennings, Nucl. Phys. **A594**, 311 (1995).
- [21] G.E. Brown and M. Rho, Nucl. Phys. **A596**, 503 (1996).
- [22] V. Koch, Phys. Lett. B **337**, 7 (1994).
- [23] M.M. Sharma, M.A. Nagarajan, and P. Ring, Phys. Lett. B **312**, 377 (1993).
- [24] M.M. Sharma, G.A. Lalazissis, and P. Ring, Phys. Lett. B **317**, 9 (1993).
- [25] N.K. Glendenning and S.A. Moszkowski, Phys. Rev. Lett. **67**, 2414 (1991).
- [26] J. Schaffner, C.B. Dover, A. Gal, C. Greiner, D.J. Millener, and H. Stoecker, Ann. Phys. (N.Y.) **235**, 35 (1994).
- [27] R. Büttgen, K. Holinde, A. Müller-Groeling, J. Speth, and P. Wyborny, Nucl. Phys. **A506**, 586 (1990).
- [28] A. Müller-Groeling, K. Holinde, and J. Speth, Nucl. Phys. **A513**, 557 (1990).
- [29] M. Hoffmann, J.W. Durso, K. Holinde, B.C. Pearce, and J. Speth, Nucl. Phys. **A593**, 341 (1995).
- [30] A. Ramos and E. Oset, in *Proceedings of Mesons and Light Nuclei, Pruhonice 1998* (World Scientific, Singapore, 1999), in press.
- [31] J.M. Eisenberg and D.S. Koltun, *Theory of Meson Interactions with Nuclei* (Wiley, New York, 1980).
- [32] T. Waas, M. Rho, and W. Weise, Nucl. Phys. **A617**, 449 (1997).
- [33] V.R. Pandharipande, C.J. Pethick, and V. Thorsson, Phys. Rev. Lett. **75**, 4567 (1995).
- [34] M. Lutz, Phys. Lett. B **426**, 12 (1998).
- [35] M. Mizoguchi, S. Hirenzaki, and H. Toki, Nucl. Phys. **A567**, 893 (1994).
- [36] K. Tsushima, K. Saito, A.W. Thomas, and S.V. Wright, Phys. Lett. B **429**, 239 (1998).

[37] J. Mareš and B.K. Jennings, Phys. Rev. C **49**, 2472 (1994).

FIGURES

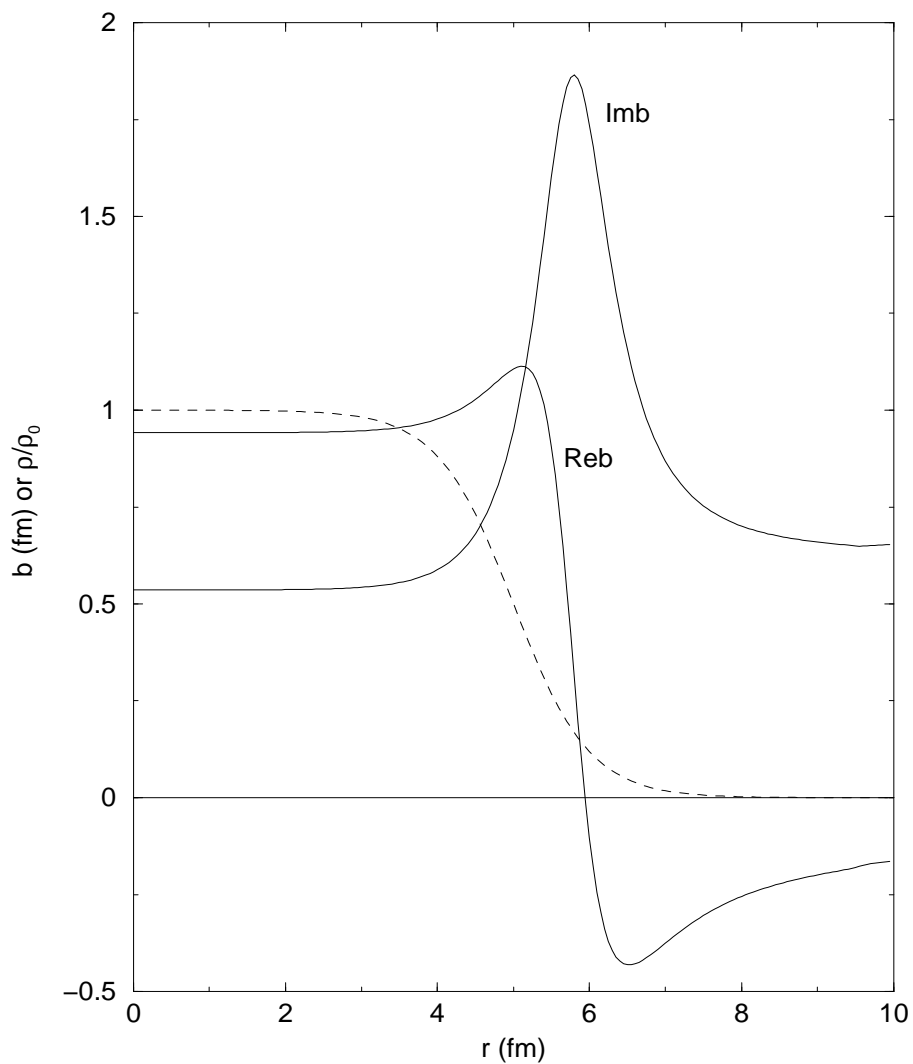


FIG. 1. Solid curves:  $b(\rho)$  from the coupled channel model [11], for a hypothetical nucleus whose density distribution is shown by the dashed curve.

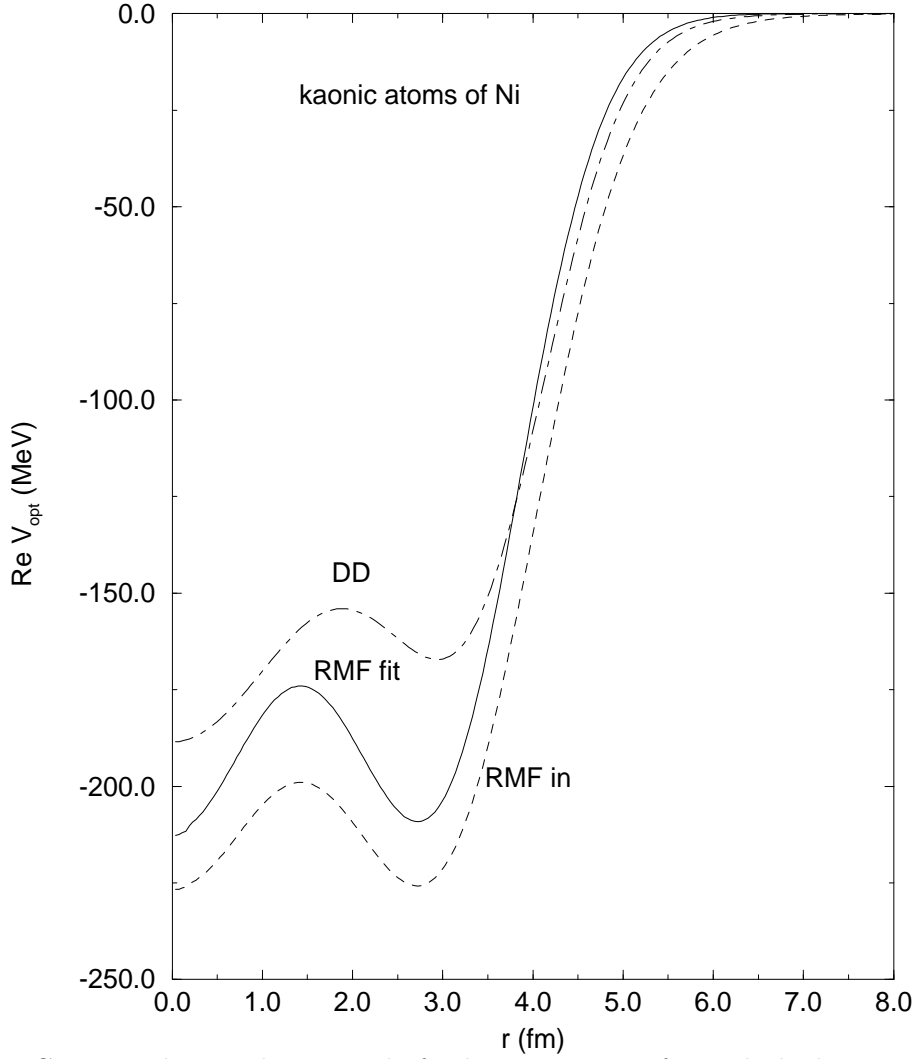


FIG. 2. Real optical potentials for kaonic atoms of Ni: dashed curve for the RMF(L) input potential (only  $\text{Im } V_{opt}$  adjusted), solid curve for the RMF(L)-adjusted potential and dot-dashed curve for the phenomenological DD potential.

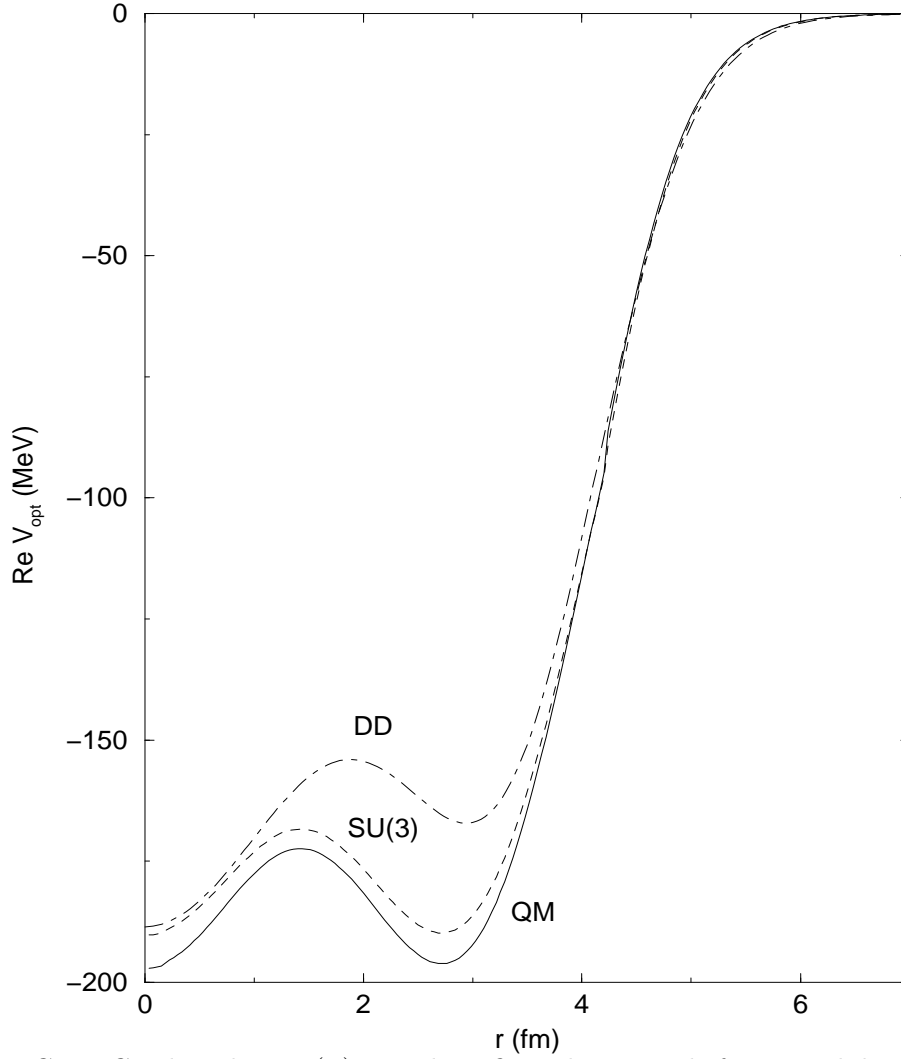


FIG. 3. Combined RMF(L)+DD best fit real potentials for Ni: solid curve for the QM version, dashed curve for the SU(3) version, see text. Also shown (dot-dashed) is the phenomenological DD potential.

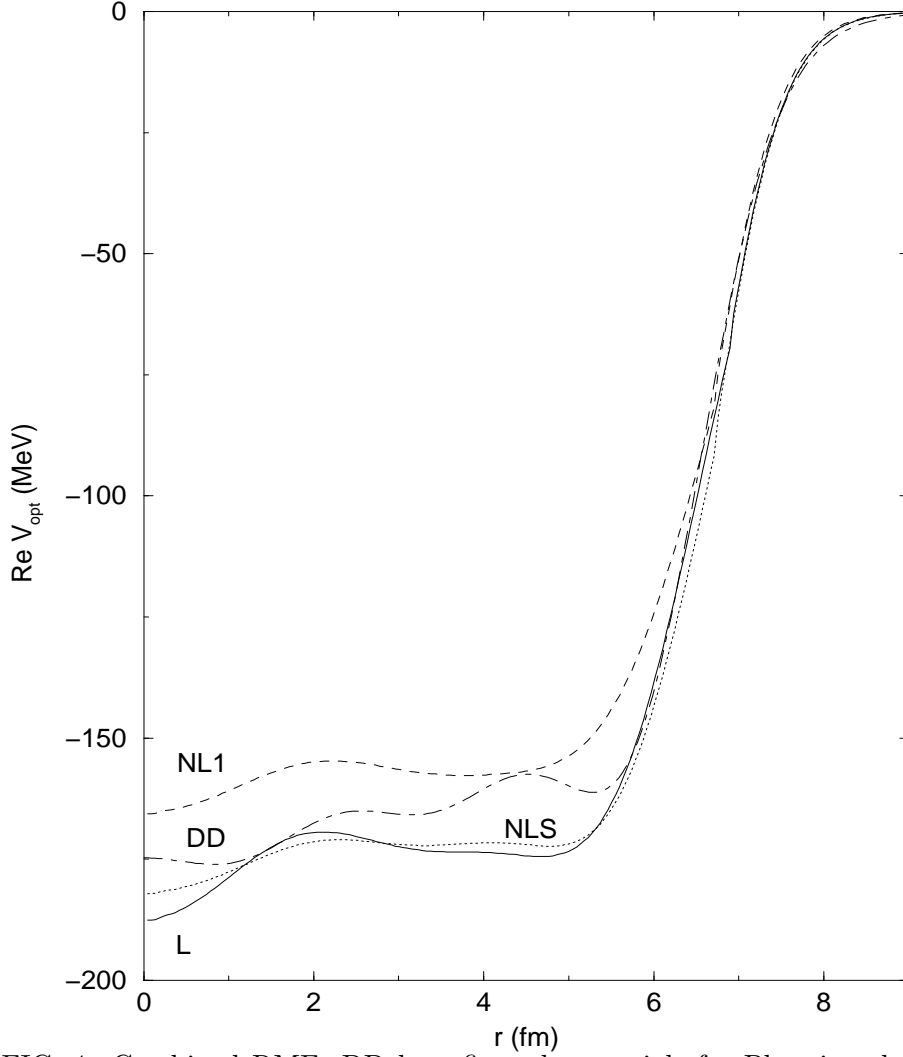


FIG. 4. Combined RMF+DD best fit real potentials for Pb using the QM version, see text. The solid curve is for model L [15], the dashed curve is for model NL1 [16] and the dotted curve is for model NLS [23]. Also shown (dot-dashed) is the phenomenological DD potential.

## TABLES

TABLE I. Parameters of the various optical potentials that fit the  $K^-$  atom data (see text).  $b_0$  and  $B_0$  are in fm, underlined quantities were held fixed during the fits,  $\alpha=1/3$  and  $0.31\pm 0.08$  for the hybrid and DD models, respectively.

	$\alpha_\omega$	$\alpha_\sigma$	$b_0$	$ReB_0$	$ImB_0$	$\chi^2/N$
RMF(L)-in	<u><math>\frac{1}{3}</math></u>	<u><math>\frac{1}{3}</math></u>	$i(1.12\pm 0.50)$	—	—	18.0
RMF(L)-fit	$0.75\pm 0.03$	$-0.73\pm 0.09$	$i(0.48\pm 0.09)$	—	—	1.53
RMF(L)+DD	<u>QM</u>	$\frac{1}{3}(0.60\pm 0.01)$	<u><math>-0.15+i0.62</math></u>	$1.95\pm 0.06$	$-0.19\pm 0.04$	1.40
RMF(NL1)+DD	<u>QM</u>	$\frac{1}{3}(0.70\pm 0.03)$	<u><math>-0.15+i0.62</math></u>	$1.78\pm 0.05$	$-0.20\pm 0.05$	1.39
RMF(L)+DD	<u>SU(3)</u>	$\frac{1}{3}(1.21\pm 0.04)$	<u><math>-0.15+i0.62</math></u>	$2.01\pm 0.06$	$-0.19\pm 0.05$	1.49
RMF(NL1)+DD	<u>SU(3)</u>	$\frac{1}{3}(1.30\pm 0.02)$	<u><math>-0.15+i0.62</math></u>	$1.83\pm 0.05$	$-0.19\pm 0.05$	1.47
DD	—	—	<u><math>-0.15+i0.62</math></u>	$1.79\pm 0.08$	$-0.22\pm 0.08$	1.28